

## Preparation and Characterization of Magnetic Molecularly Imprinted Polymers for Selective Recognition of 3-Methylindole

Dandan Niu,<sup>1</sup> Zhiping Zhou,<sup>1</sup> Wenming Yang,<sup>1</sup> Yuan Li,<sup>2</sup> Li Xia,<sup>1</sup> Bo Jiang,<sup>2</sup> Wanzhen Xu,<sup>2</sup> Weihong Huang,<sup>2</sup> Tingyang Zhu<sup>1</sup>

<sup>1</sup>Department of Materials Science and Engineering, Jiangsu University, Zhenjiang 212013, People's Republic of China

<sup>2</sup>Department of Environment, Jiangsu University, Zhenjiang 212013, People's Republic of China

Correspondence to: Z. Zhou (E-mail: zhouzp@ujs.edu.cn)

**ABSTRACT:** In this work, magnetic molecularly imprinted polymers (MMIPs) were used as novel adsorbents for selective adsorption of 3-methylindole from model oil. The MMIPs were synthesized by precipitation polymerization and surface molecularly imprinted technique, using Fe<sub>3</sub>O<sub>4</sub> nanoparticles as magnetically susceptible component, methylacrylic acid as dressing agent and functional monomer, ethylene glycol dimethacrylate as crosslinker, and 3-methylindole as template molecule. The MMIPs were characterized by Fourier-transform infrared spectroscopy, scanning electron microscopy, vibrating sample magnetometer, and thermogravimetric analyzer, respectively. The adsorption performances of MMIPs were investigated by batch adsorption experiments in terms of kinetics, isotherms, and selective recognition adsorption, respectively. The results indicate that MMIPs have high recognition ability and fast binding kinetics for 3-methylindole. Meanwhile, the adsorption equilibrium time was about 2 h and the equilibrium adsorption amount was  $\sim 38 \text{ mg g}^{-1}$  at 298 K. The heterogeneous MMIPs were modeled with pseudo-second-order and Langmuir isotherm equation. © 2013 Wiley Periodicals, Inc. *J. Appl. Polym. Sci.* 000: 000–000, 2013

**KEYWORDS:** adsorption; functionalization of polymers; molecular recognition; separation techniques

Received 7 December 2012; accepted 3 May 2013; Published online 00 Month 2013

**DOI:** 10.1002/app.39511

### INTRODUCTION

The organic nitrogen compounds in the fuel can be converted to nitrogen oxides (NO<sub>x</sub>) through combustion, which have an adverse effect on the environment, such as air pollution and acid rain.<sup>1–3</sup> These nitrides, including pyridine, quinoline, and indole, reduce the quality of fuel and poison the catalyst in further processing.<sup>4</sup> Thereby, nitrides in the fuel must be removed as much as possible before being combusted.

Conventional denitrogenation technologies have a few limitations in petrochemical industry due to some drawbacks. For example, hydrodenitrogenation method is costly and difficult to control under operating conditions of high pressure and temperature;<sup>5–7</sup> Coordination extraction method can move organic nitrides completely, but metal ion salts, used as extractant, are inconvenient for denitrogenation;<sup>8,9</sup> Biological denitrogenation method is high-priced even though it is quick and efficient. So, it is a significant research topic to develop a novel denitrogenation technology in petrochemical industry.<sup>10,11</sup>

Molecularly imprinted polymers (MIPs) are powerful materials to make imprinted cavities within a polymer network. It is rooted in antibody theory put forward by Pauling. MIPs were synthesized

for the first time by Wulff in 1973 and developed rapidly since then. Theophylline imprinted MIPs were prepared by Mosbach in 1993.<sup>12</sup> MIPs are polymerized by functional monomer which has specific functions with template molecule. It would form idiosyncratic bonding sites which are complementary with template molecule in shape and chemical functional groups if it is eluted by physical or chemical methods. The technique of MIPs has attracted attention recently for its exceptional benefits such as predetermined recognition ability, stability, comparatively easy and low cost of preparation.<sup>13–16</sup> In recent years, MIPs have been applied in many fields. Luo et al.<sup>14</sup>, Kohei et al.,<sup>16</sup> and Brüggemann et al.<sup>17</sup> have reported that MIPs were used as adsorbent to remove contaminants from aqueous environment. Liu, H.<sup>18</sup> extracted uric acid from herbs by MIPs. A voltammetric sensor for albumin, which combined the techniques of microfabrication and molecular imprinting, was investigated by Hui et al.<sup>19</sup> Imprinted polymer catalysts show obvious catalytic properties in Oliver's work.<sup>20</sup> Imprinting technology could impact directly in enhanced drug loading of controlled-release carriers for the sustained release of therapeutic agents.<sup>21</sup>

However, the traditional MIPs have some drawbacks still, including permanent entrapment of the template, unfavorable

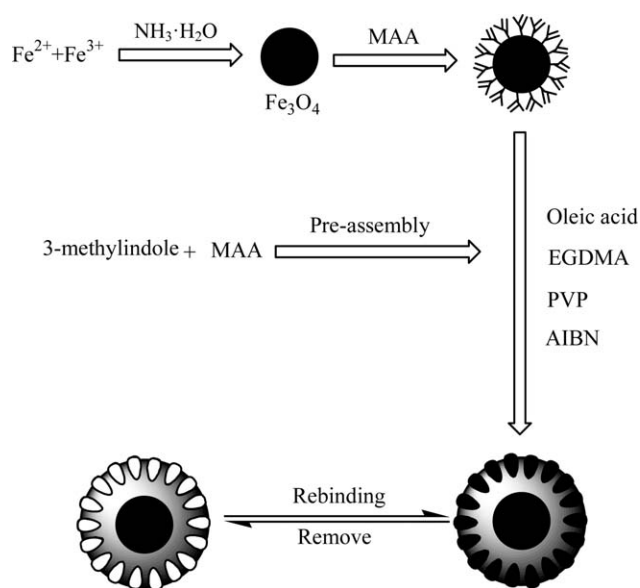


Figure 1. Schematic illustration of synthesis procedure of MMIPs.

kinetics of the adsorption and desorption process, and so on. Based on these disadvantages of MIPs, the surface MIPs were introduced with great advantages, such as steerable size due to controllable matrix materials and skin thickness, better mechanism and good reuse performance owing to decreasing embedding of adsorption site and increasing adsorption driving force.<sup>22,23</sup> Magnetic separation technology has received considerable attention because it can be performed directly in crude sample, which is especially useful for rapid application and large-scale operation. Magnetic nanoparticle is brought in as matrix materials to separate adsorbent from samples easily. Magnetic molecularly imprinted polymers (MMIPs) had been reported in the literature,<sup>23–28</sup> which integrate the merits of surface MIPs and magnetic nanoparticles.

In this work, to realize the selection adsorption to 3-methylindole, the MMIPs were synthesized by precipitation polymerization with the supporter of modified magnetic nanoparticles. First,  $\text{Fe}_3\text{O}_4$  was synthesized by coprecipitation method and was modified by methylacrylic acid (MAA). Then, polymers were anchored on the surface of modified magnetic nanoparticles. The properties of MMIPs were characterized by Fourier transform infrared (FTIR) spectroscopy, scanning electron microscopy (SEM), vibrating sample magnetometer (VSM), and thermogravimetric analyzer (TGA), respectively. In the adsorption experiment, the MMIPs were separated from the model oil by an external field, and the suspension was analyzed by gas chromatography (GS) methods. Furthermore, adsorption data were analyzed by kinetic and isotherm models.

## EXPERIMENTAL

### Chemicals

Indole (98.5%), 3-methylindole (98%), quinoline (99%), benzothiophene (99%), ethyl glycol dimethacrylate (EGDMA, 98%), and MAA were all purchased from the Aladdin Chemical (Shanghai, P. R. China, www.aladdin-e.com). All the reagents

employed, including toluene, glacial acetic acid, methanol, ethanol, *n*-octane, 2,2'-azobisisobutyronitrile (AIBN),  $\text{FeCl}_2 \cdot 4\text{H}_2\text{O}$ ,  $\text{FeCl}_3 \cdot 6\text{H}_2\text{O}$ , ammonium hydroxide (25%), oleic acid, polyvinylpyrrolidone (PVP), were supplied by the Sinopharm Chemical Reagent (Shanghai, P. R. China, www.sinoreagent.com.cn). Water used in the experiments was redistilled water.

### Synthesis and Surface Modification of $\text{Fe}_3\text{O}_4$ Nanoparticles

The synthesis process of  $\text{Fe}_3\text{O}_4$  magnetic nanoparticles refers to literature.<sup>29</sup> The black precipitate was separated by a permanent magnet and washed for several times by  $\text{H}_2\text{O}$  and ethanol, respectively. Magnetic fluid was prepared by the addition of 100 mL ethanol into washed  $\text{Fe}_3\text{O}_4$ . The process of surface modification was as follows: 50 mL magnetic fluid and 70 mL ethanol were dispersed into a three-necked flask (250 mL). The mixture was stirred and purged with nitrogen gas. MAA (8 mL) was added when the temperature reached to 70°C. The reaction was maintained for 24 h. The product  $\text{Fe}_3\text{O}_4$ -MAA was separated by a permanent magnet. Then, it was washed for several times by ethanol and dried in the vacuum oven at 60°C.

### Synthesis of 3-Methylindole MMIPs

The MMIPs were synthesized by the improved method reported by Pan et al.<sup>30</sup> Template molecular is linked together with functional monomer through hydrogen bonding and dehydrated solvent was used in this work. The steps are listed as follows:

- 3-Methylindole (131.18 mg) and MAA (0.68 mL) were dissolved in toluene (30 mL). This mixture was stirred for 30 min for preparation of the pre-assembly solution.
- $\text{Fe}_3\text{O}_4$ -MAA (0.3 g) was blended with 2.0 mL of oleic acid and 6.8 mL of EGDMA, and the mixture was stirred in ultrasonic bath for 1 h. Then the preassembly solution was added into the mixture and was stirred for another 30 min for preparation of the pre-polymerization.
- PVP (0.4 g) was dissolved into 150 mL of toluene in a three-necked flask. The mixture was stirred in nitrogen atmosphere when the temperature reached to 60°C. Then pre-polymerization solution and AIBN, as initiator, were added into the flask. The reaction was kept under 60°C for 24 h.
- The polymerization product was separated from the mixture by magnet and was washed with methanol/ethanol acid (3 : 7, v/v) by Soxhlet extraction till the template molecule could not be detected by GS spectrophotometer. Then the polymers were washed with water for several times again and were dried at 60°C in a vacuum. As a control, the magnetic nonimprinted polymers (MNIPs) were prepared also by the same synthetic procedure except for the absence of template molecules. Figure 1 shows the schematic illustration of synthesis procedure of MMIPs.

### Characterizations of MMIPs

GC was performed with an Agilent 7890A (Varian Instruments, Palo Alto, CA) system comprising a flame ionization detector. Infrared spectrums of the composite nanoparticles were taken by a Nicolet Nexus 470 FTIR spectrometer (Thermo Fisher Scientific). The surface morphology of samples was observed by SEM (JSM-7001F). Magnetic measurements were carried out using a VSM (HH-15, Nanjing University) at room

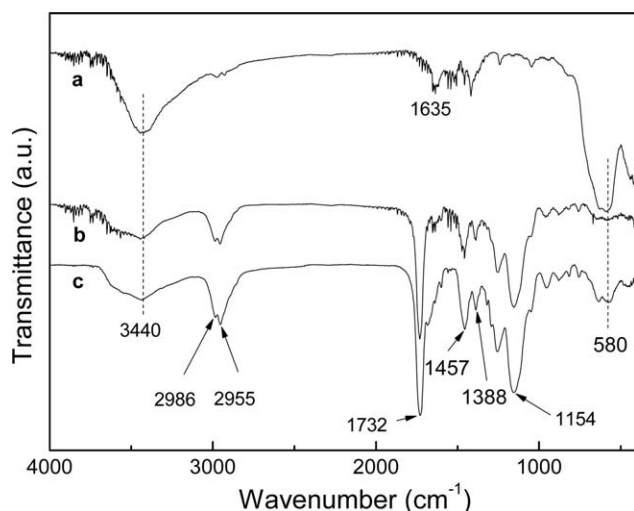


Figure 2. FTIR spectra of Fe<sub>3</sub>O<sub>4</sub>-MAA (a), MMIPs (b), and MNIPs (c).

temperature. The chemical content of MMIPs was characterized by TGA (STA449C).

#### Adsorption Experiments

Kinetics adsorption, isothermal adsorption, and selective adsorption were carried out to evaluate the recognition properties of MMIPs. The influences of initial concentration, equilibration time, and temperature option on the adsorption of 3-methylindole were investigated. In the study of adsorption experiments, 6 mL of aqueous solutions was adsorbed with 10 mg of adsorbents in batch experiments. The mixture was vibrated in a temperature-controlled air shaker. And then the supernatant and adsorbent were separated by magnet. Finally, concentration of the supernatant was determined by GC. The kinetics adsorption experiments were calculated at the temperature of 298, 308 and 318 K with the concentration of 300 in different time ranging from 5 to 180 min. Isothermal adsorption experiments were tested at the temperature of 298, 308, and 318 K with initial concentration ranging from 100 to 500 mg L<sup>-1</sup> for 3 h to reached adsorption balance. The adsorption selectivity experiments were carried out by MMIPs and MNIPs at 298 K with the concentration of 300 mg L<sup>-1</sup> for 3 h to reach adsorption balance. The adsorption capacity was calculated by a mass balance relationship:

$$Q_e = \frac{V(C_0 - C_e)}{m} \quad (1)$$

where  $C_0$  (mg L<sup>-1</sup>) is the initial concentration of 3-methylindole,  $C_e$  (mg L<sup>-1</sup>) is the 3-methylindole concentration of the supernatant solution,  $V$  (L) is the volume of the initial solution, and  $m$  (g) is the mass of adsorbent.

## RESULTS AND DISCUSSION

### Characterizations

FTIR spectra were obtained for Fe<sub>3</sub>O<sub>4</sub>-MAA, MMIPs, and MNIPs, respectively. As shown in Figure 2, the characteristic bands around 580 cm<sup>-1</sup> show the existence of Fe—O group

stretching vibration.<sup>27</sup> The peak at 1635 cm<sup>-1</sup> in Fe<sub>3</sub>O<sub>4</sub>-MAA belongs to the C=C stretching vibrations<sup>31</sup> which testifies that MAA was grafted on the surface of Fe<sub>3</sub>O<sub>4</sub>. MMIPs and MNIPs have some new peaks, for example, peaks at 1732 cm<sup>-1</sup> (C=O stretching vibrations) and 1154 cm<sup>-1</sup> (C—O stretching vibrations), which are attributed to MAA and EGDMA. The peaks at 2986 and 2955 cm<sup>-1</sup> indicate the presence of C—H stretching vibrations of both —CH<sub>3</sub> and —CH<sub>2</sub>— groups. Meanwhile, the peaks at 1388 and 1457 cm<sup>-1</sup> give another proof of the existence of —CH<sub>3</sub> and —CH<sub>2</sub>— groups. Moreover, the broad band at 3440 cm<sup>-1</sup> indicates that the surface of Fe<sub>3</sub>O<sub>4</sub>-MAA, MMIPs, and MNIPs have many OH groups. All results confirm that the polymerization of MAA and EGDMA initiated by AIBN on the surface of Fe<sub>3</sub>O<sub>4</sub>-MAA is successful.

TGA was applied to quantify the amount of polymers and that of Fe<sub>3</sub>O<sub>4</sub> enclosed in MMIPs. The thermogravimetric analysis (TGA) curves of Fe<sub>3</sub>O<sub>4</sub>-MAA (a) and MMIPs (b) were given in Figure 3. There is no decrease in weight of Fe<sub>3</sub>O<sub>4</sub>-MAA between 25 and 100°C, which shows the samples to be utterly dried. The weight loss of MMIPs before 100°C is 5.60%, which is mainly due to moisture evaporation caused by inadequate drying. The loss of Fe<sub>3</sub>O<sub>4</sub>-MAA after 100°C is 5.39%, which is caused by MAA grafted on the surface of Fe<sub>3</sub>O<sub>4</sub>. The large weight loss of MMIPs is 89.00%, and it shows that it started to decompose at 235°C. Thus, the remaining mass of Fe<sub>3</sub>O<sub>4</sub>-MAA and MMIPs belongs to Fe<sub>3</sub>O<sub>4</sub>, which cannot melt until 1594.5°C. These reach a conclusion that the quantity of Fe<sub>3</sub>O<sub>4</sub> in the MMIPs is 5.40%.

SEM was used to study the detailed morphology of MMIPs and MNIPs. As shown in Figure 4, MMIPs particles are ~5 μm in diameter and some of MMIPs aggregate together. The outward appearance of eluted MMIPs is different from that of MNIPs. In addition, the MMIPs have a rough surface and lots of holes, while MNIPs possess less porous. The morphology of MMIPs and MNIPs depends on the type of crosslinking monomer, initiator, solvent, temperature, and time. Meanwhile, the size and shape of both MMIPs and MNIPs are irregular, which may be

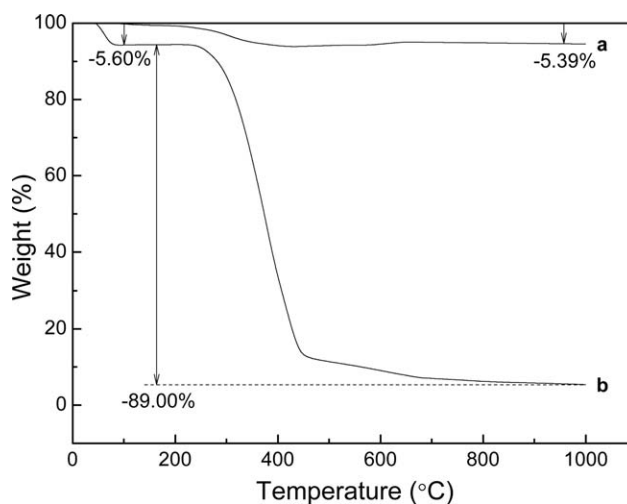


Figure 3. TGA curves of Fe<sub>3</sub>O<sub>4</sub>-MAA (a) and MMIPs (b).

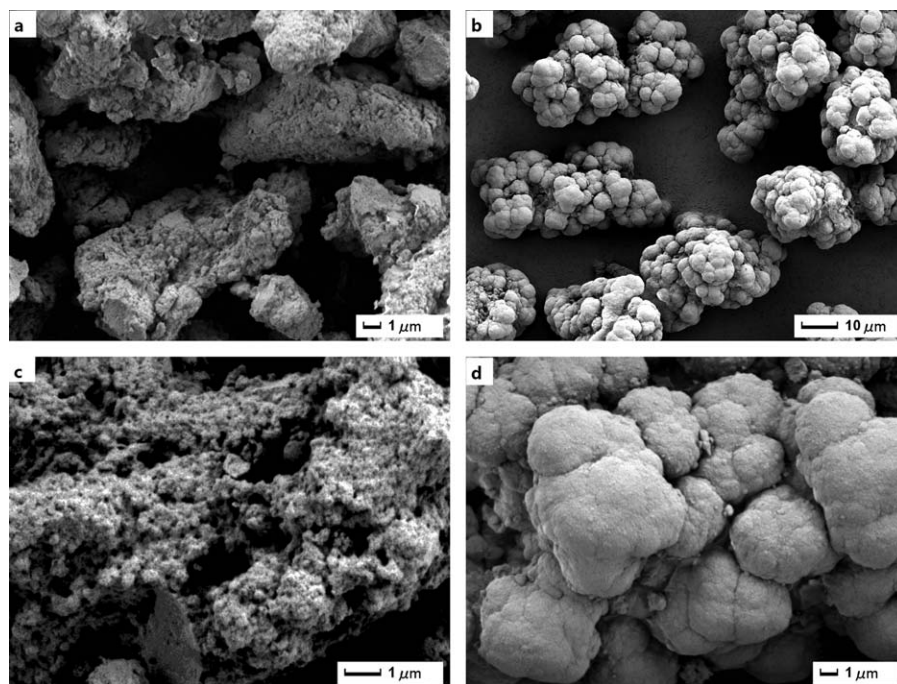


Figure 4. SEM images of MMIPs (a,c) and MNIPs (b,d).

attributed to the tiny difference of stirring speed and the process of elution.

Figure 5 shows the magnetic hysteresis loops of  $\text{Fe}_3\text{O}_4$ -MAA and MMIPs, respectively. It is obvious that there is no hysteresis in the magnetization curves of the two samples. Moreover, the magnetic curves are symmetrical and pass accurately through the origin, suggesting that both the remanence and coercivity are zero. These results suggest that MMIPs are superparamagnetic, which facilitates magnetic separation. The saturation magnetization values of  $\text{Fe}_3\text{O}_4$ -MAA and MMIPs are 46.7 and 13.1  $\text{emu g}^{-1}$ , respectively. The decreased magnetization value of MMIPs is attributed to the shielding of polymeric coating.

#### Adsorption Kinetics

For 3-methylindole, the adsorption kinetics of MMIPs was studied by the static equilibrium adsorption. The adsorption results were shown in Figure 6. The adsorption amount of 3-methylindole increases sharply in the early 40 min, and then it changes slightly. Finally, it reaches to an equilibrium state. The equilibrium adsorption amount is 38.3  $\text{mg g}^{-1}$  at 298 K. Compared with our previous work, the values of  $Q_e$  of MMIPs for 3-methylindole are more excellent than that of dibenzothio- phene reported by Li et al.<sup>31</sup> Since hydrogen bond interaction decreases with increasing temperature, the equilibrium adsorption capacity at 298 K is more outstanding than that at 303 and 313 K in this work, which is opposed to that reported by Xu et al.<sup>32</sup> and Pan et al.<sup>33</sup>

In this study, the pseudo-first-order and pseudo-second-order model<sup>34,35</sup> were applied to investigate the controlling mechanism of the adsorption of 3-methylindole onto MMIPs. The pseudo-first-order equation, which assumes that diffusion is the

rate-limiting step in the adsorption process, can be expressed as follows:

$$\ln(Q_e - Q_t) = \ln Q_e - k_1 t \quad (2)$$

The pseudo-second-order equation, which based on the assumption that the rate-limiting step may be chemical adsorption involving valency forces through sharing or exchange of electrons between adsorbent and adsorbate, can be expressed as follows:

$$\frac{t}{Q_t} = \frac{1}{k_2 Q_e^2} + \frac{t}{Q_e} \quad (3)$$

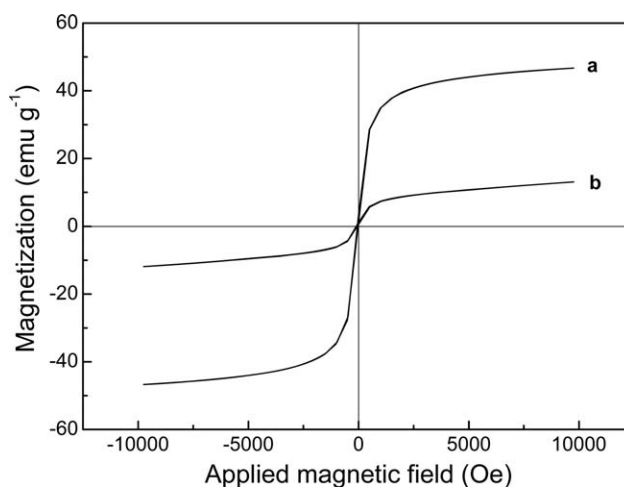
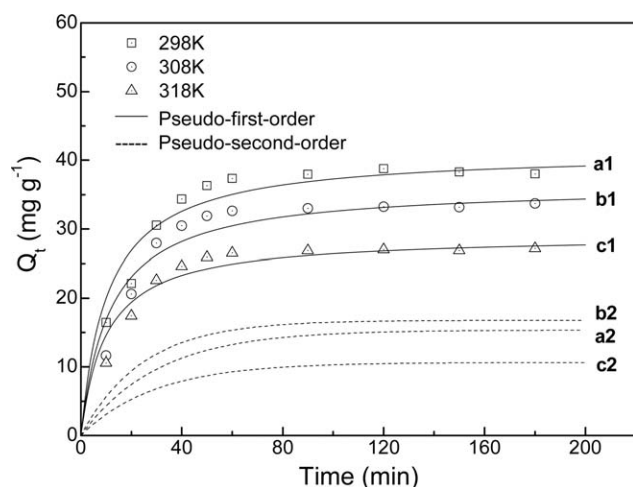


Figure 5. Magnetization curves of  $\text{Fe}_3\text{O}_4$ -MAA (a) and MMIPs (b).



**Figure 6.** Kinetics models of the effect of temperature and adsorption time for 3-methylindole onto MMIPs.

where  $Q_e$  and  $Q_t$  are the amount of adsorbate ( $\text{mg g}^{-1}$ ) onto adsorbent at the equilibrium state and time  $t$  (min), respectively;  $k_1$  ( $\text{L min}^{-1}$ ) and  $k_2$  ( $\text{g mg}^{-1} \text{min}^{-1}$ ) refer to the rate constant of the pseudo-first-order and pseudo-second-order model, which may be calculated from the plot of  $\ln(Q_e - Q_t)$  versus  $t$  and  $t/Q_t$  versus  $t$ , respectively.

The applicability of the models was studied by judging standard deviation ( $\Delta q$ , %):

$$\Delta q = \sqrt{\frac{\sum [(Q_{\text{exp}} - Q_{\text{cal}}) / Q_{\text{exp}}]^2}{N - 1}} \times 100\% \quad (4)$$

where  $q_{\text{exp}}$  and  $q_{\text{cal}}$  ( $\text{mg g}^{-1}$ ) are experimental and calculated amount of 3-methylindole adsorbed on MMIPs, respectively, and  $N$  indicates the number of data points in the experimental data.

All the adsorption rate constants and linear regression correlation coefficients were presented in Table I. The  $Q_{e,\text{cal}}$  of pseudo-first-order model gives poorer fitting with  $Q_{e,\text{exp}}$  than those calculated by pseudo-second-order model. In addition, the values of correlation coefficient ( $R^2$ ) of pseudo-second-order model are closer to 1 than that of pseudo-first-order model. Moreover, the value of  $\Delta q$  for pseudo-second-order model is lower than that for pseudo-first-order. These data illustrate that pseudo-second-order model is more suitable to describe the adsorption kinetics process than pseudo-first-order model. Meanwhile, the

fitting curves of pseudo-second-order and pseudo-second-order model were shown in Figure 6. It can be seen clearly that the pseudo-second-order fits well with experimental data. That is to say, the pseudo-second-order model is more suitable to describe the adsorption kinetics than pseudo-first-order, indicating that the rate-limiting step may be chemical process in the adsorption process for 3-methylindole.

Based on the pseudo-second-order kinetic model, the initial adsorption rate,  $h$  ( $\text{mg g}^{-1} \text{min}^{-1}$ ), and adsorption half-time,  $t_{1/2}$  (min),<sup>32,33</sup> were calculated by the equations:

$$h = k_2 Q_e^2 \quad (5)$$

$$t_{1/2} = \frac{1}{k_2 Q_e} \quad (6)$$

The adsorption rate can be measured in terms of initial adsorption rate and adsorption half-time. The results were summarized in Table I. These data indicate that initial adsorption rate decreases and the adsorption half-time changes slightly with increasing temperature.

#### Adsorption Isotherm

The adsorption isotherm was used to communicate affinity and adsorption capacity of adsorbent. The adsorption results were shown in Figure 7. The adsorption amount of 3-methylindole onto MMIPs increases with the increase of initial concentration, while it decreases with increasing temperature. It is caused by adsorption driving force, namely hydrogen bond force and difference in concentration. The higher the temperature, the lower adsorption sites bond 3-methylindole, and the lower adsorption amount are. At the same time, higher concentration can provide more adsorption driving force and enhance adsorption amount.

The experimental data were analyzed by three isotherm models.<sup>32</sup> Based on the monolayer adsorption model, Langmuir isotherm equation was put forward:

$$Q_e = \frac{K_L Q_m C_e}{1 + K_L C_e} \quad (7)$$

Freundlich isotherm model<sup>23,36</sup> assumes that the adsorbent has asymmetrical surface morphology. Freundlich isotherm equation is:

$$Q_e = K_F C_e^{1/n} \quad (8)$$

**Table I.** Kinetics Constants of Pseudo-First-Order and Pseudo-Second-Order Equation

Temp. (K)	$Q_{e,\text{exp}}$ ( $\text{mg g}^{-1}$ )	Pseudo-first-order				Pseudo-second-order					
		$Q_{e,\text{cal}}$ ( $\text{mg g}^{-1}$ )	$k_1 \times 10^2$ ( $\text{min}^{-1}$ )	$R^2$	$\Delta q$ (%)	$Q_{e,\text{cal}}$ ( $\text{mg g}^{-1}$ )	$k_2 \times 10^3$ ( $\text{g mg}^{-1} \text{min}^{-1}$ )	$R^2$	$\Delta q$ (%)	$h$ ( $\text{mg g}^{-1} \text{min}^{-1}$ )	$T_{1/2}$ (min)
298	38.3	15.36	3.305	0.7434	68.51	41.25	2.273	0.9947	10.80	3.869	10.663
308	33.3	16.77	4.103	0.8661	55.55	36.32	2.387	0.9929	16.28	3.149	11.535
318	27.1	10.64	3.407	0.7869	69.15	29.04	3.464	0.9951	13.83	2.922	9.940

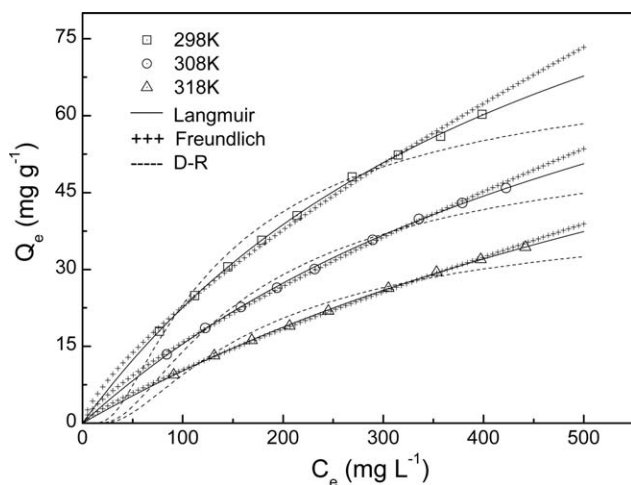


**Figure 7.** Isotherm models of the effect of temperature and initial concentration for 3-methylindole onto MMIPs.

The Dubinin–Radushkevich (D-R) equation is used to describing the adsorption behavior onto heterogeneous surfaces. It can be expressed as follows:

$$\ln Q_e = \ln Q_m - \beta \varepsilon^2 \quad (9)$$

where  $Q_e$  ( $\text{mg g}^{-1}$ ),  $Q_m$  ( $\text{mg g}^{-1}$ ), and  $C_e$  ( $\text{mg L}^{-1}$ ) are adsorbed amount, theoretical maximum adsorption capacity and concentration of 3-methylindole at equilibrium state, respectively;  $K_L$  ( $\text{L mg}^{-1}$ ),  $K_F$  ( $\text{mg g}^{-1}$ ), and  $\beta$  are Langmuir constant, Freundlich constant and D-R constant, which can be calculated from the plot of  $C_e/Q_e$  versus  $C_e$ ,  $\ln Q_e$  versus  $\ln C_e$  and  $\ln Q_e$  versus  $\varepsilon^2$ , respectively;  $n$  is Freundlich constant relating to the affinity between adsorbent and adsorbate;  $\varepsilon$  is Polanyi potential given as follows:

$$\varepsilon = RT \ln \left( 1 + \frac{1}{C_e} \right) \quad (10)$$

where  $R$  is the gas constant;  $T$  is the temperature in K.

All constants of three isotherm models were shown in Table II. It suggests that a rising in adsorption temperature results in the decrease of  $K_L$  and  $Q_m$  in Langmuir model.  $K_F$  decreases and  $1/n$  changes slightly with increasing temperature in Freundlich model. In addition, the value of  $\Delta q$  for Langmuir model is lower than that for Freundlich and D-R model. The simulated curves were exhibited in Figure 7. It can be seen clearly that

**Table II.** Isotherm constants of Langmuir, Freundlich, and D-R equation

Temp. (K)	Langmuir				Freundlich				D-R			
	$Q_m$ ( $\text{mg g}^{-1}$ )	$K_L \times 10^3$ ( $\text{L mg}^{-1}$ )	$R^2$	$\Delta q$ (%)	$K_F$ ( $\text{mg g}^{-1}$ )	$1/n$	$R^2$	$\Delta q$ (%)	$Q_m$ ( $\text{mg g}^{-1}$ )	$\beta \times 10^3$	$R^2$	$\Delta q$ (%)
298	135.14	2.008	0.9979	0.63	0.8002	0.7271	0.9946	2.81	51.74	1.17	0.8452	15.11
308	116.96	1.525	0.9955	0.87	0.4774	0.7595	0.9981	1.72	39.16	1.43	0.8303	16.10
318	111.24	1.012	0.9937	0.76	0.2424	0.8171	0.9988	1.43	29.10	1.76	0.8275	17.11

**Table III.** Thermodynamic Parameters for Adsorption of 3-Methylindole onto MMIPs

Temp. (K)	$\Delta G$ ( $\text{Kj mol}^{-1}$ )	$\Delta H$ ( $\text{kJ mol}^{-1}$ )	$\Delta S$ ( $\text{J mol}^{-1} \text{K}^{-1}$ )
298	-13.881	-26.925	-43.801
308	-13.568	-26.925	-43.801
318	-12.925	-26.925	-43.801

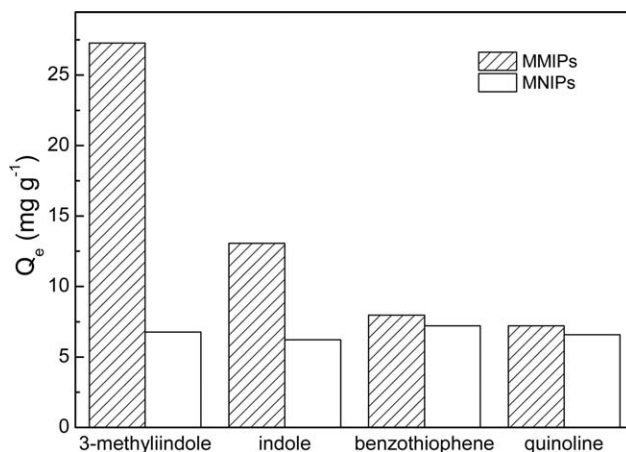


**Figure 8.** Selective adsorption of 3-methylindole, indole, benzothiophene, and quinoline.

Langmuir isotherm model corresponds to experimental data better both in low and high concentration. These results indicate Langmuir model is suitable to describe the adsorption isotherm, suggesting that the adsorption of 3-methylindole onto MMIPs is monomolecular chemical adsorption.

#### Adsorption Thermodynamics

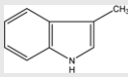
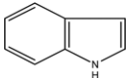
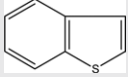
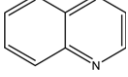
Thermodynamic parameters can be calculated according to the thermodynamic equilibrium constants in different temperature.<sup>31</sup> The Gibbs free energy ( $\Delta G$ ), enthalpy change ( $\Delta H$ ), and entropy change ( $\Delta S$ )<sup>32</sup> were computed by the following equations where  $K_L$  was used as constant:

$$\Delta G = -RT \ln K_L \quad (11)$$

$$\ln K_L = \frac{-\Delta H}{RT} + \frac{\Delta S}{R} \quad (12)$$

The calculated values of thermodynamic parameters were reported in Table III. The negative values of  $\Delta H$  show that the

**Table IV.** Distribution Coefficient and Selectivity Coefficient Data

Analytes	Chemical Formula	$Q_e$ (mg g <sup>-1</sup> )		$K_d$		$k$		$k'$
		MMIPs	MNIPs	MMIPs	MNIPs	MMIPs	MNIPs	
3-Methylindole		27.275	6.773	0.185	0.040	-	-	-
Indole		13.075	6.211	0.089	0.040	2.072	0.996	2.081
Benzothiophene		7.978	7.210	0.062	0.055	2.991	0.726	4.120
Quinoline		7.214	6.576	0.042	0.038	4.433	1.064	4.165

nature of adsorption process is exothermic. The negative value of  $\Delta S$  can be explained by the decreased degree of randomness due to the hydrogen bonding of 3-methylindole onto active sites of MMIPs. The negative value of  $\Delta G$  indicates that the adsorption process is spontaneous.

#### Adsorption Selectivity

In this section, the unique selective recognition of MMIPs towards 3-methylindole was investigated by calculating adsorption amount of 3-methylindole and its structural analogues. The structural analogues such as 3-methylindole, quinoline, and benzothiophene were chosen as the reference compounds in mixed solution. The experimental adsorption data of MMIPs and MNIPs were shown in Figure 8. It can be clearly seen that the adsorption amount of 3-methylindole onto MMIPs is more outstanding than that of its structural analogues due to the idiosyncratic bonding sites. In addition, the adsorption amount of MMIPs is more than that of MNIPs towards 3-methylindole because of the deficiency of bonding sites on the surface of MNIPs. Moreover, the adsorption amounts of structural analogues onto MMIPs and MNIPs are poor and similar to each other.

Static distribution factor ( $K_d$ ), separation factor ( $k$ ), and relative separation factor ( $k'$ ),<sup>23,32,36</sup> used to evaluate the selectivity of MMIPs, were calculated according to eq. (13)–(15):

$$K_d = \frac{C_p}{C_s} \quad (13)$$

$$k = \frac{K_{d1}}{K_{d2}} \quad (14)$$

$$k' = \frac{k_{\text{MMIPs}}}{k_{\text{MNIPs}}} \quad (15)$$

where  $C_p$  is the adsorbed concentration, while  $C_s$  is the concentration of supernatant;  $K_{d1}$  and  $K_{d2}$  are static distribution coefficients of 3-methylindole and its structural analogues, respectively;  $k_{\text{MMIPs}}$  and  $k_{\text{MNIPs}}$  are the separation factors of

MMIPs and MNIPs, respectively. The experimental data and parameters were summarized in Table IV. It is evident that the values of  $Q_e$  and  $k_d$  of MMIPs for 3-methylindole are more excellent than that of MNIPs. In addition, the values of  $k'$  of indole, benzothiophene, and quinoline show less differentiation, which may be led by the similar functional groups and molecular structure between 3-methylindole and its structural analogues. All these confirm that MMIPs had a strong ability to 3-methylindole compared with other structural analogues in mixed solution.

#### CONCLUSIONS

MMIPs, based on modified Fe<sub>3</sub>O<sub>4</sub> nanoparticles, were successfully synthesized by precipitation polymerization for selective adsorption of 3-methylindole from model oil solution. The obtained MMIPs were characterized by FTIR, SEM, VSM, and TGA. Adsorption experiments were measured by batch process. The pseudo-second-order kinetic model provides the best description, suggesting that chemical process is the rate-limiting step in the adsorption process. Experimental data are in good agreement with the Langmuir isotherm model, which means that the adsorption process is monomolecular adsorption. The thermodynamic parameters indicate that the adsorption is an exothermic and spontaneous process. Furthermore, MMIPs show outstanding selectivity to 3-methylindole, compared with its structural analogues. We believe that the magnetic surface-molecularly imprinted technique can be one of the most promising candidates for denitrogenation of fuel oil in the future.

#### REFERENCES

1. Kwon, J. M.; Moon, J. H.; Bae, Y. S.; Lee, D. G.; Sohn, H. C.; Lee, C. H. *Chem. Sus. Chem.* **2008**, *1*, 307.
2. Wojtowicz, M. A.; Pels, J. R.; Moulijn, J. A. *Fuel* **1994**, *73*, 9.
3. Williams, A.; Pourkashanian, M.; Jones, J. M.; Rowlands, L. J. I. *Energy* **1997**, *70*, 102.
4. Yu, D. Y.; Xu, H.; Que, G. H. *Technol. Progr.* **2001**, *10*, 32.
5. Ojeda, J.; Escalona, N.; Fierro, J. L. G. A.; López, A.; Gil-Llambías, F. J. *Appl. Catal. A* **2005**, *281*, 25.

6. Chen, W. Y.; Chen, Y. L.; Zhang, H. B.; Xinjiang. *Oil. Gas.* **2010**, *6*, 74.
7. Chu, Y. J.; Wei, Z. B.; Yang, S. W.; Li, C.; Xin, Q.; Min, E. *Z. Appl. Catal. A* **1999**, *176*, 17.
8. Atsushi, I.; Wang, D. H.; Franck, D. *Appl. Catal. A* **2005**, *279*, 279.
9. Eun, S. H.; Alexey, Z.; Jelliarko, P. *Energ. Fuel* **2009**, *23*, 3032.
10. Li, W. L.; Xing, J. M.; Xiong, X. C. *Eng. Chem. Res.* **2006**, *45*, 2845.
11. Rafael, V. D.; Eduardo, T.; Brenda, V. *Energ. Fuel* **2002**, *16*, 1239.
12. Makoto, K.; Toshifumi, T.; Takashi, M.; Hiroyuki, A. *Molecular Inprinting: From Fundamentals to Applications*; Science Press: Beijing, **2006**; Vol. 1, Chapter 2, pp 6–13.
13. Wang, X. J.; Xu, Z. L.; Feng, J. L. *J. Membr. Sci.* **2008**, *313*, 97.
14. Luo, X. B.; Deng, F.; Luo, S. L.; Tu, X. M.; Yang, L. X. *J. Appl. Polym. Sci.* **2011**, *121*, 1930.
15. Huang, J. T.; Zheng, S. H.; Zhang, J. Q. *Polymer* **2004**, *45*, 4349.
16. Kohei, T.; Masanori, A.; Takaomi, K. *J. Appl. Polym. Sci.* **2005**, *97*, 620.
17. Brüggemann, O.; Visnjeviski, A.; Burch, R.; Patel, P. *Anal. Chim. Acta.* **2004**, *504*, 81.
18. Liu, H. M.; Liu, C. H.; Yang, X. J. *Anal. Chim. Acta.* **2008**, *628*, 87.
19. Hui, C. H.; Chin, I. L.; Abraham, K. J.; Yu, D. L. *J. Chromatogr. A.* **2004**, *1027*, 263.
20. Oliver, B. *Anal. Chim. Acta.* **2001**, *435*, 197.
21. Zachary, J. H.; Mark, E. B. *Adv. Drug. Delivery Rev.* **2004**, *56*, 1599.
22. Li, L.; He, X. W.; Chen, L. X.; Zhang, Y. K. *Chem. Asian. J.* **2009**, *4*, 286.
23. Guo, W. H.; Hu, W.; Pan, J. M. *Chem. Eng. J.* **2011**, *171*, 603.
24. Hu, Y. L.; Liu, R. J.; Zhang, Y.; Li, G. K. *Talanta* **2009**, *79*, 576.
25. Ding, M. J.; Wu, X. L.; Yuan, L. H. *J. Hazard. Mater.* **2011**, *191*, 177.
26. Li, Y.; Ding, M. J.; Wang, S. *Appl. Mater. Int.* **2011**, *3*, 3308.
27. Jing, T.; Du, H. R.; Dai, Q. *Biosens. Bioelectron.* **2010**, *26*, 301.
28. Liu, Y. L.; Huang, Y. Y.; Liu, J. Z. *J. Chromatogr. A.* **2012**, *1246*, 15.
29. Olga, P.; Anna, B.; Vyacheslav, M.; Alesci, K. *Eur. Polym. J.* **2011**, *47*, 542.
30. Pan, J. M.; Xu, L. C.; Dai, J. D. *Chem. Eng. J.* **2011**, *174*, 68.
31. Li, H.; Xu, W. Z.; Wang, N. W. *Microchim. Acta* **2012**, *179*, 123.
32. Xu, W. Z.; Zhou, W.; Huang, W. H. *Microchim. Acta.* **2011**, *175*, 167.
33. Pan, J. M.; Yao, H.; Xu, L. C. *J. Phys. Chem. C.* **2011**, *115*, 5440.
34. Yuh, S.; Augustine, E. O. *J. Hazard. Mater.* **2006**, *129*, 137.
35. Ho, Y. S.; McKay, G. *Process Biochem.* **1999**, *34*, 451.
36. Liu, Y.; Liu, Z. C.; Wang, Y. *Microchim. Acta.* **2011**, *172*, 309.